Signatures of quantum criticality in hole-doped and chemically pressurized $EuFe_2As_2$ single crystals

Jannis Maiwald,* H. S. Jeevan, and Philipp Gegenwart
I. Physikalisches Institut, Georg-August-Universität Göttingen, D-37077 Göttingen, Germany
(Received 1 November 2011; revised manuscript received 20 December 2011; published 5 January 2012)

We study the effect of hole doping and chemical pressure (isovalent doping) in single crystals of $K_xEu_{1-x}Fe_2As_2$ and $EuFe_2(As_{1-y}P_y)_2$, respectively, by measuring the thermopower, $S(T)$, and electrical resistivity, $\rho(T)$. The evolution of $S(T)$ upon doping indicates drastic changes in the electronic configuration at critical values $x_{cr} = 0.3$ and $y_{cr} = 0.21$, respectively, as the spin-density-wave transition is completely suppressed and superconductivity (SC) emerges. For the case of chemical pressure, a comparison with published ARPES measurements indicates a Lifshitz transition at y_{cr}. The temperature dependences $S(T)/T \propto \log T$ and $\Delta\rho \propto T$ observed in the normal state above the SC transition suggest quantum criticality in both systems.

DOI: 10.1103/PhysRevB.85.024511 PACS number(s): 05.30.Rt, 74.70.Xa, 74.20.Mn, 74.25.fg

I. INTRODUCTION

Unconventional superconductivity (SC) often occurs in systems with multiple competing phases and fluctuations.[1] In particular, it has been demonstrated for heavy-fermion metals that SC is maximal at the point where long-range magnetic order disappears.[2] Such a quantum critical point (QCP) leads to strong magnetic fluctuations in its vicinity in the phase diagram, which may act as glue for unconventional SC. It is therefore very important to characterize quantum critical behavior in the normal state of unconventional superconductors.

In this paper, we focus on a possible QCP in the vicinity of the SC phase of the iron pnictide $EuFe_2As_2$.[3] This system belongs to the so-called "122" family of the recently discovered iron pnictides: MFe_2As_2 (M = divalent alkaline earth or rare earth metal: Ca, Sr, Ba, and Eu). In order to induce SC in this compound, the spin-density-wave (SDW)–type antiferromagnetic (AF) ordering of FeAs layers with $T_{SDW} = 189$ K needs to be suppressed. This can generally be achieved in two ways: application of external pressure or chemical substitution of either K or Na to the Eu site (hole doping) or P to the As site (isovalent substitution).[3–7] The suppression of the AF order occurs continuously, thus the system is a candidate for a potential QCP. Due to the localized $4f$ moments of the Eu atoms, the system is the only 122 compound that features a second magnetic sublattice. The corresponding Eu^{2+} moments order AF around 19 K. However, the coupling between the two magnetic sublattices is weak.[8,9]

The 122-type iron pnictides feature a complex fermiology, consisting of three hole-like Fermi surfaces (h-FSs) at the center of the first Brillouin zone [$\mathbf{\Gamma}$ point; $\mathbf{k} = (0,0)$] and two electron-like Fermi surfaces (e-FSs) at the corner [$\mathbf{M}$ point; $\mathbf{k} = (\pi,\pi)$]. The two e-FSs and the two inner h-FSs are basically two-dimensional (2D), while the outer h-FS has a more three-dimensional (3D) character due to a stronger dispersion along $\mathbf{k}_z$.[10–12] The SDW ordering takes place along the nesting vector $\mathbf{Q}_n$ in the $\mathbf{\Gamma}$-$\mathbf{M}$ direction. Upon hole doping, the h-FSs expand, while the e-FSs shrink along the k_xk_y plane. This leads to a weakening of the nesting condition and hence to a suppression of the SDW ordering. On the other hand, the isovalent substitution of As with the smaller P leads to a substantial reduction in the unit-cell volume. Recent *angle-resolved photoemission spectroscopy* (ARPES) measurements on $EuFe_2(As_{1-y}P_y)_2$ showed that the e-FSs stay almost unchanged, while the h-FSs become more 3D, because P substitution leads to a drastic reduction in the c/a ratio,[13] enhancing the dispersion along k_z.[14] The stronger warping of the h-FSs breaks the nesting condition and eventually leads to SC.[15]

In the case of iron pnictides, a possible QCP is hidden by SC and therefore indications of quantum critical behavior are limited to temperatures above $T_c \approx 35$ K. Since the specific heat at this temperatures is highly dominated by the phonon contribution and (in our case) the contribution of Eu^{2+} moments, it is not possible to analyze non-Fermi-liquid (NFL) behavior in this property. Instead, we focus on the thermoelectric power, $S(T)$, which has recently been shown to be a very sensitive probe of quantum criticality.[16] While thermopower divided by temperature, $S(T)/T$, is constant for a Landau Fermi liquid, a logarithmic divergence, $S/T \propto \log T$, is expected in the quantum critical regime for a 2D SDW QCP.[16] Note that these temperature dependences are similar to those expected for the specific heat coefficient C/T. Furthermore, we analyze the temperature dependence of the electrical resistivity, for which the same model predicts a linear temperature dependence,[17] in sharp contrast to the T^2 behavior characteristic for Landau Fermi liquids.

The paper is organized as follows: Sec. II provides information on the single-crystal synthesis and characterization, while thermopower and electrical resistivity results on $K_xEu_{1-x}Fe_2As_2$ and $EuFe_2(As_{1-y}P_y)_2$ are discussed in Sec. III A and III B, respectively. This is the first study on single crystals of a former hole-doped system, while the phase diagram for isovalent P substitution has been determined on single crystals previously.[13,18]

II. METHODS

A series of $K_xEu_{1-x}Fe_2As_2$ single crystals was synthesized using the self-flux method, in which the crystals grow out of an FeAs flux. In the first step, precursors of FeAs and KAs were synthesized using simple solid-state reactions. Stoichiometric amounts of the respective starting elements (Fe, 99.998%; As, 99.999%; K, 99.95%) were placed in an Al_2O_3 crucible, which was then sealed in a Ta crucible under an argon

atmosphere. The FeAs batch was heated to 600°C at the rate of 100°C/h for 10 h, followed by heating to a temperature of 700°C at the rate of 50°C/h for 20 h, and was then quickly (250°C/h) cooled to room temperature. The KAs batch was slowly heated to 700°C at the rate of 25°C/h and kept there for 6 h, after which it was also cooled to room temperature quickly.

Stoichiometric amounts (as for a 1:4:4 compound) of FeAs, KAs, and Fe powder were thoroughly mixed with small pieces of Eu (99.99%) and then sealed as described above. All steps had to be carried out under an argon atmosphere to prevent the highly reactive materials KAs and Eu from reacting with the air. Single crystals of $K_xEu_{1-x}Fe_2As_2$ were then grown by heating the batches under various temperature profiles. The most successful one regarding the composition and size of the crystals was as follows: heating at a rate of 50°C/h to 1100°C, maintenance of this temperature for a total of approximately 4 h, followed by actual growth, caused by decreasing the temperature at a rate of 3°C/h down to 900°C. Afterward the temperature was quickly reduced to room temperature. Using this method we were able to grow large plate-like single crystals with a typical dimension of 4×3 mm^2 in the *ab* plane. Single crystals of $EuFe_2As_2$ and $EuFe_2(As_{1-y}P_y)_2$ were grown using a Bridgman method.[8,13]

Structural characterization of the obtained single crystals was done by Laue diffraction and powder x-ray diffraction. The Laue method confirmed the single-crystalline character of the samples. The diffraction patterns of all investigated crystals could be indexed using the $ThCr_2Si_2$ tetragonal-type structure (space group: I4/*mmm*). Some samples exhibited a small amount of Fe_2As impurity phase. This amount was estimated to be less than 4%. Chemically the crystals were characterized with a scanning electron microscope equipped with energy-dispersive x-ray analysis on the freshly cleaved surfaces. The inhomogeneity within the *ab* plane was found to be around 1%. However, we found interlayer inhomogeneities along the *c* axis which could become substantial ($\leqslant$15%). Therefore, the crystals were chosen very carefully and cleaved as thin as possible in order to reduce the error due to these interlayer inhomogeneities. Further characterization was performed by measuring the specific heat and the magnetic susceptibility of the specimens.

In general, we found that doping the Eu site with K was very difficult, probably due to the very different chemical properties of Eu and K. The potassium tends to leave the Al_2O_3 crucible and reacts with the tantalum. Even an excess of 2 times the nominal value had almost no effect on the concentration of measured crystals. Therefore, the measured doping concentrations did not exceed $x = 0.52$.

Electrical resistivity, specific heat, magnetic susceptibility, and thermoelectric power were measured by standard Quantum Design PPMS and MPMS systems. The contacts for thermopower measurements were made with ordinary copper wires and a two-component epoxy, which was cured at a temperature of 150°C for 10 min in an open furnace. The contact resistance was usually found to be less than 1 Ω. Samples were then mounted on the measurement puck in a standard four-probe configuration, as described in the Thermal Transport Option User's Manual of the PPMS.[19]

III. RESULTS

A. $K_xEu_{1-x}Fe_2As_2$

Figure 1 displays the phase diagram of $K_xEu_{1-x}Fe_2As_2$ as obtained from electrical resistivity and magnetic susceptibility measurements on various different single crystals. Both T_{SDW}, due to Fe magnetic ordering, and T_N, due to Eu magnetic ordering, lead to changes in the slope of $\rho(T)$ [cf. Fig. 3(a)], similar to the previous findings with polycrystalline samples.[3] As in other iron pnictides, the SDW transition is accompanied by a structural lattice distortion, which changes the crystal structure from tetragonal to orthorhombic (space group: C*mma*). We could not resolve any splitting of these transitions in our experiments. With doping, the SDW order is continuously suppressed down to approximately $T_{SDW} \approx 160$ K, where it eventually vanishes, suggesting that the SDW state might be limited to the Eu-rich region of the phase diagram. For $x > 0.3$, the SDW transition is completely suppressed and SC develops with a maximal $T_c \approx 34$ K near $x = 0.5$. Magnetic susceptibility data shown in Fig. 2 provide evidence for bulk SC in this concentration regime. We note that the broad resistive transition at $x = 0.22$ (cf. Fig. 3) is probably not due to bulk SC but, rather, due to a minor volume fraction of higher x (see Sec. II), which has a negligible influence on the normal state properties. The data in Fig. 2 also indicate at least a partial AF ordering of diluted Eu^{2+} moments within the SC state. When the optimal doping is exceeded, T_c seems to decrease again. It is probable that SC is not fully suppressed with further doping, since the end member of this doping series KFe_2As_2 shows SC, with a transition temperature of $T_c = 3.4$ K.[20]

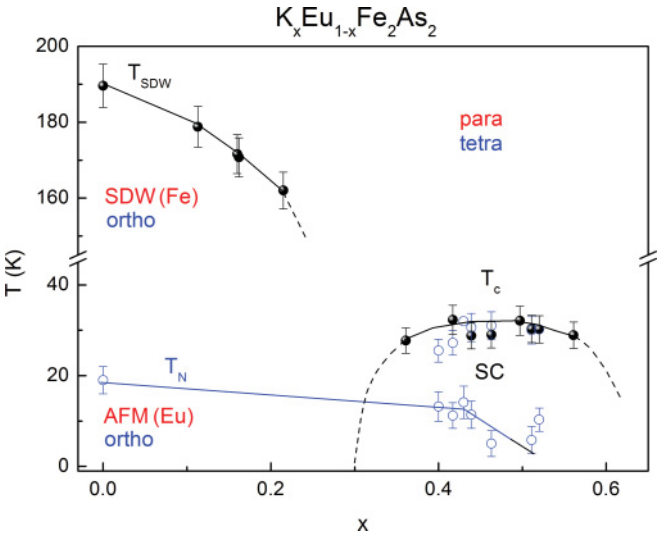

FIG. 1. (Color online) Phase diagram for $K_xEu_{1-x}Fe_2As_2$ as a function of x. Filled (black) circles represent phase transition temperatures obtained from resistivity measurements, while transition temperatures [open (blue) circles] are derived from susceptibility measurements. Solid lines act as guides for the eye, and dashed lines are extrapolations using the available experimental data.

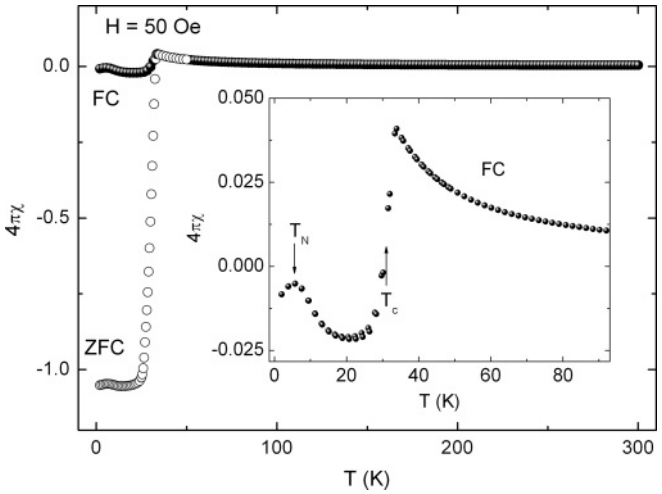

FIG. 2. Magnetic susceptibility of $K_xEu_{1-x}Fe_2As_2$ with $x = 0.51$ vs temperature. Filled and open circles represent data obtained in a field of 50 Oe during field-cooled (FC) and zero-field-cooled (ZFC) measurements. Inset: FC data at low temperatures. Upward- and downward-pointing arrows mark T_c and T_N, respectively.

1. Analysis of electrical resistivity

The power-law behavior of the resistivity data for various compositions was analyzed systematically, using a three-parameter fit function, $\rho(T) = \rho_0 + AT^n$, to extract the effective exponent, n. Figure 3(a) shows the resistivity data for some selected compositions. The validity of the fit is shown by the dashed lines. The resistivity exponent as a function of doping is shown in Fig. 3(b). With increasing K doping, n decreases linearly until it reaches a minimum value of 1 at $x = 0.51$. The exponent then starts to increases again with further doping. Such NFL behavior with exponent $n = 1$ would be compatible with a 2D SDW QCP. Very similar behavior has previously been found in K-doped $SrFe_2As_2$ polycrystals.[21]

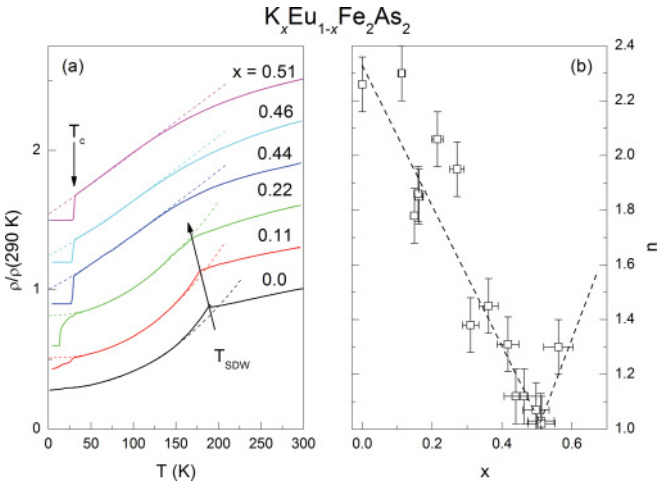

FIG. 3. (Color online) (a) Electrical resistivity $\rho(T)/\rho(290\ \mathrm{K})$ vs temperature for various $K_xEu_{1-x}Fe_2As_2$ single crystals. Note, that the data are offset by 0.3, respectively. Dashed lines indicate $\rho(T) = \rho_0 + AT^n$ dependence. (b) Derived evolution of the exponent n vs x.

2. Thermoelectric power

The thermoelectric power S is usually the sum of the drift thermopower S_{drift}—which is caused by charge separation due to a thermal gradient—and the phonon drag thermopower S_{drag}—which has its origin in the electron-phonon interaction. S_{drag} can be either a positive or a negative contribution to the total thermopower, depending on various factors such as the fermiology, distance of the FS to the Brillouin zone boundary, dominating scattering process (normal process, Umklapp process), etc.[22,23]

Figure 4 depicts the thermopower measurements as a function of temperature for several doping compositions. At high temperatures the thermoelectric power of the parent compound $EuFe_2As_2$ exhibits a roughly constant positive value of approximately 7μV/K. This might indicate that the dominant carriers are hole-like in this temperature range. However, the investigated compound is a multiband system which consists of three hole-like Fermi surfaces at the $\mathbf{\Gamma}$ point and two electron-like FSs at the $\mathbf{M}$ point. The thermopower is therefore composed of different contributions from all these bands, making a general statement difficult. Nevertheless, this interpretation seems to be supported by Hall effect measurements, which show a positive Hall coefficient above 190K.[24] Approaching the SDW transition $S(T)$ exhibits a strong increase leading to a pronounced maximum, peaking around 150 K. A similar signature has previously been found, e.g., in the Ca-122 system.[25] At temperatures below 50 K the thermopower crosses over to negative values and exhibits a minimum, which is centered around the Néel temperature of the system. However, this feature is also present in other systems (Ba-122, Sr-122, Cs-122, K-122, and even La-1111)[26–30] and can therefore not be related to the ordering of the Eu^{2+} moments. Using the reported Debye temperatures Θ_D of the various systems, we find that the temperature at which the minimum in S is found corresponds to $\Theta_D/6$. This value is well within the limits for a phonon drag peak ($\Theta_D/5$, $\Theta_D/10$).[22,23] We therefore propose that the observed feature

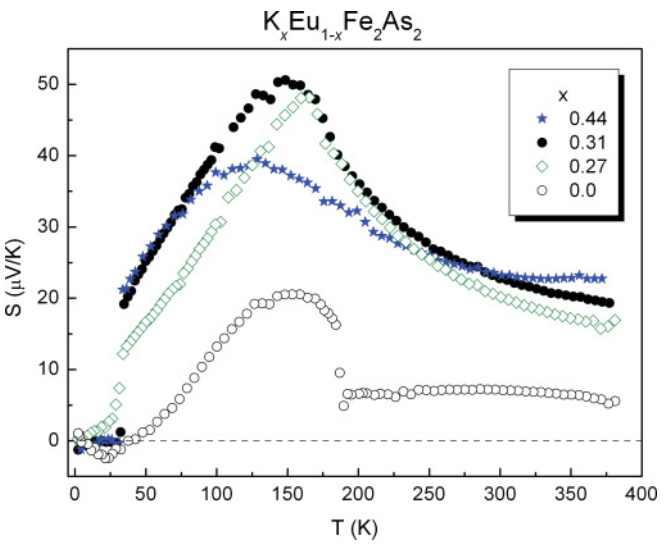

FIG. 4. (Color online) Thermoelectric power S vs temperature for various $K_xEu_{1-x}Fe_2As_2$ single crystals. The dashed line marks $S = 0$.

is attributed to a negative S_{drag} contribution, which greatly decreases the value of $S(T)$ below 150 K and leads to the observed minimum around 20 K.

The size of the thermoelectric power at room temperature increases monotonically with increasing K doping and reaches large values, of the order of 25 μV/K. Qualitatively, the increase in S with increasing hole doping is expected in a simple rigid band picture. Such behavior in the evolution of the band structure is already known for hole-doped Ba-122 and Sr-122.[15] On the other hand, band structure calculations for the $K_xBa_{1-x}Fe_2As_2$ system have questioned the rigid band model, indicating that the main effect of doping is a change in the relative sizes of the FSs as a consequence of the change in As height with doping.[31] At the same time, the peak associated with the SDW transition gets broader, confirming observations in resistivity measurements, where the SDW transition in a $\partial\rho/\partial T$ plot broadened with doping (not shown). The maximum value of the thermopower, $S_{max}(x)$, increases rapidly with hole doping and peaks at the critical composition $x_{cr} = 0.3$, as shown in Fig. 5(a). With further doping, S_{max} decreases. A similar behavior has been found in K-doped Sr-122 polycrystals.[32] The thermopower at fixed temperatures as a function of the control parameter, $S(x)|_{T=const}$, also exhibits an anomalous behavior at the same composition [Fig. 5(b)]. Similar signatures have recently been observed in Co- and Ru-doped $BaFe_2As_2$.[33] The signatures at $x_{cr} = 0.3$, i.e., at the composition where the SDW order is fully suppressed and SC emerges (cf. Fig. 1), indicate significant changes in the electronic structure of the system.

We now focus on the indications of quantum criticality in the temperature dependence of the thermoelectric power. As shown in Fig. 6, the $x = 0.44$ sample, which is located close to the optimum concentration for SC, displays a logarithmic divergence in S/T over a substantial temperature range. Similar behavior was observed in K-doped Sr-122 polycrystals.[21]

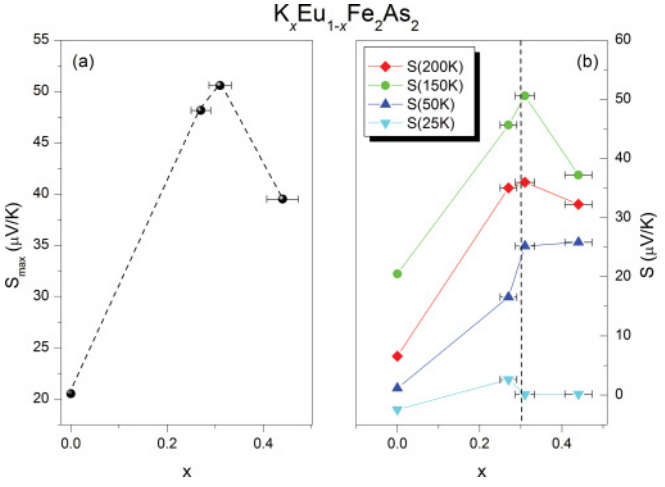

FIG. 5. (Color online) (a) Maximum values of the thermoelectric power S vs K concentration derived from various $K_xEu_{1-x}Fe_2As_2$ single crystals. (b) S vs K concentration for several temperatures. The dashed line in (a) acts as a guide for the eye, while in (b) it shows the critical composition $x_{cr} = 0.3$.

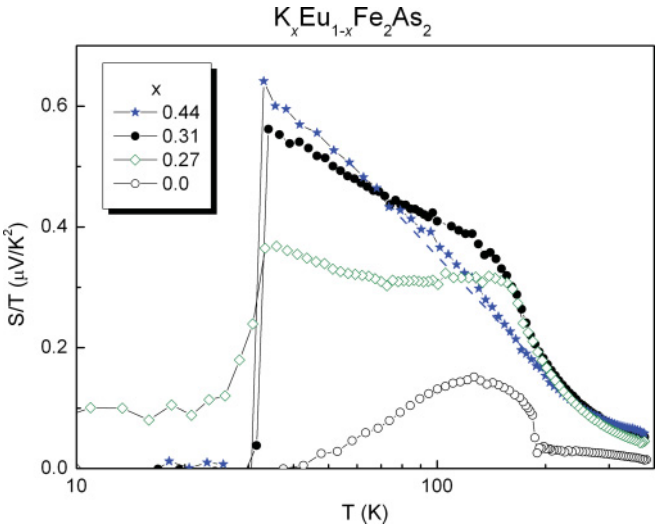

FIG. 6. (Color online) Thermoelectric power divided by temperature S/T vs temperature (on a logarithmic scale) for various single crystals of $K_xEu_{1-x}Fe_2As_2$. The dashed line acts as a guide for the eye.

B. $EuFe_2(As_{1-y}P_y)_2$

The phase diagram of $EuFe_2(As_{1-y}P_y)_2$ has previously been determined by resistivity, magnetic susceptibility, and specific heat measurements.[13] Remarkably, SC is confined to a very narrow regime ($0.16 \leqslant y \leqslant 0.22$), beyond which a ferromagnetic Eu^{2+} ordering acts detrimentally. Below, we focus on thermoelectric power measurements on similar single crystals. As shown in Fig. 7, the evolution of $S(T)$ is distinctly different from that found for $K_xEu_{1-x}Fe_2As_2$.

At room temperature, S decreases with increasing P substitution and changes sign at $y = 0.21$. In an oversimplified picture this would indicate a shift from holes to electrons as the dominant carrier type. Samples with $y > 0.21$ show a negative thermopower over the whole temperature range below 300 K,

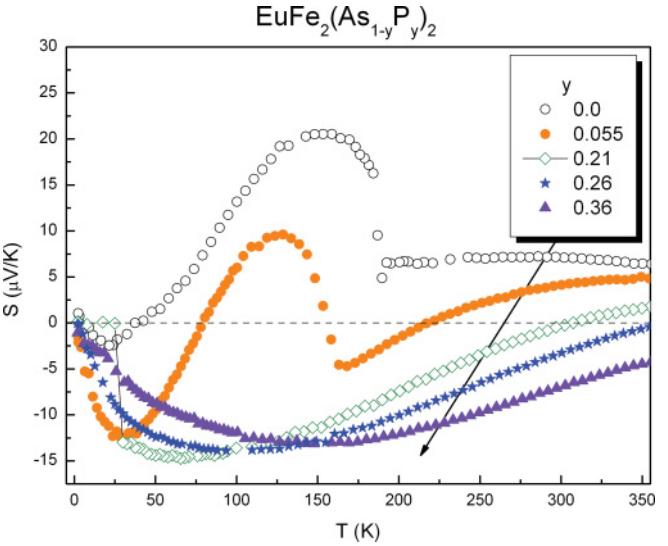

FIG. 7. (Color online) Thermoelectric power S vs temperature for various $EuFe_2(As_{1-y}P_y)_2$ single crystals. The dashed line marks $S = 0$, while the arrow indicates the increase in P concentration.

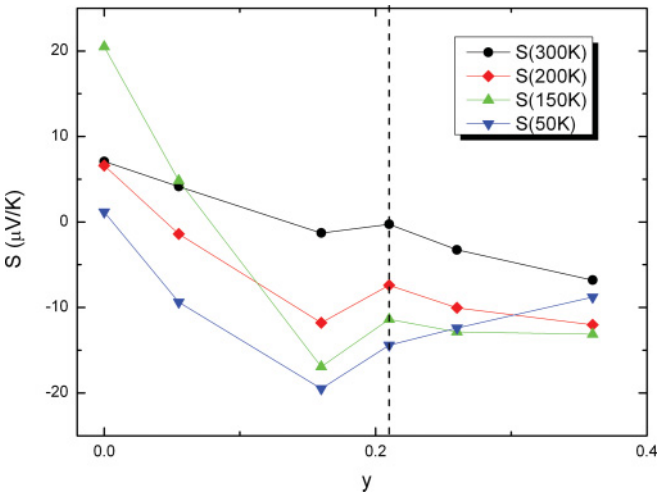

FIG. 8. (Color online) Thermoelectric power S vs P concentration derived from various single crystals of $EuFe_2(As_{1-y}P_y)_2$. The dashed line indicates the critical composition $y_{cr} = 0.21$.

with a broad minimum at lower temperatures. The crossover from positive to negative values leads to distinct sign changes in the $y = 0.055$ crystal, for which T_{SDW} is reduced to about 150 K.

The evolution of the thermopower with P substitution, plotted in Fig. 8, indicates a distinct signature at $y_{cr} = 0.21$. This is close to the concentration at which SC is suppressed.[13] At this composition, ARPES measurements from Thirupathaiah *et al.* also revealed a Lifshitz transition related to the vanishing of the inner h-FS at the Γ point.[14] Recently, Liu *et al.* proposed that a necessary condition for SC in Co-doped Ba-122 is a nonreconstructed central hole pocket, rather than a perfect nesting condition between the central and the corner pockets.[34] Our data seem to be in agreement with this proposal.

Finally, we address signatures of NFL behavior in the thermopower and electrical resistivity. Similar to the case of

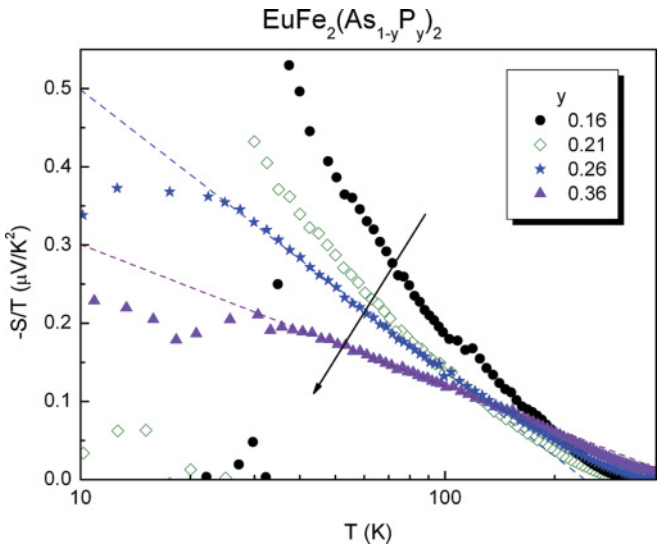

FIG. 9. (Color online) Thermoelectric power divided by temperature S/T vs temperature (on a logarithmic scale) for various single crystals of $EuFe_2(As_{1-y}P_y)_2$. Dashed lines act as a guide for the eye, while the arrow indicates the increase in P concentration.

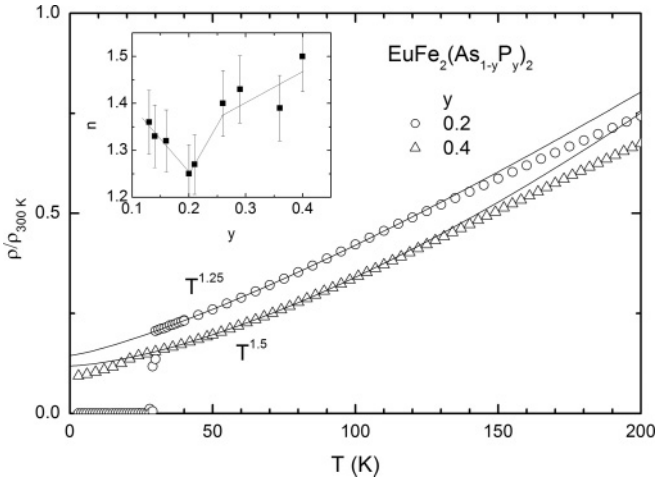

FIG. 10. Electrical resistivity $\rho(T)/\rho(300\ \mathrm{K})$ vs temperature for two single crystals of $EuFe_2(As_{1-y}P_y)_2$ (data from Ref. 13). Lines indicate $\rho(T) = \rho_0 + AT^n$ dependence. Inset: Evolution of the exponent $n(y)$ for various $EuFe_2(As_{1-y}P_y)_2$ single crystals.

the hole-doped system, the temperature dependence of S/T also indicates a substantial regime (approximately one decade in T) for which a logarithmic divergence is observed (cf. dashed lines in Fig. 9). Most singular behavior (even weak power-law divergence) is found at low P concentrations, while with increasing y, the increase in $-S/T$ upon cooling is weaker, suggesting that the QCP is located close to $y_{cr} = 0.21$.

Similarly to the hole-doped system, the electrical resistivity data on P-substituted single crystals from Ref. 13 could also be described by a power-law function, $\rho(T) = \rho_0 + AT^n$, at temperatures between 30 and 120 K (cf. Fig. 10), with exponent $n < 2$ indicative of NFL behavior. The evolution of $n(y)$ displays a clear minimum at $y \approx 0.2$, providing additional evidence for a QCP close to y_{cr}. Interestingly, the minimal value of the resistivity exponent is about 1.25, which is significantly higher than the $n = 1$ found for the case of hole-doped $K_{0.5}Eu_{0.5}Fe_2As_2$. This may suggest that the critical magnetic fluctuations likely responsible for these NFL effects are less 2D (more isotropic) in the P-substituted case.

IV. CONCLUSION

We have grown, for the first time, single crystals of the series $K_xEu_{1-x}Fe_2As_2$ and investigated their bulk properties, with particular emphasis on changes in the electronic structure and possible indications for quantum criticality. With increasing hole doping, the thermopower at room temperature increases monotonically toward very large values. The electrical resistivity data suggest NFL behavior near $x = 0.5$. This is supported by the observation of a logarithmic divergence in the thermoelectric power coefficient S/T. Similar indications are also found in single crystals of $EuFe_2(As_{1-y}P_y)_2$. Here, the P substitution acts as chemical pressure and suppresses the nesting properties of the FS by pushing the dimensionality of the band structure toward 3D. With increasing y, the thermoelectric power becomes negative and displays a pronounced minimum at low temperatures. We associate this minimum, which is also present in other iron pnictide systems at the respective Debye temperatures, with a large phonon drag

contribution. Furthermore, we observe a distinct signature in the thermopower evolution at $y_{cr} = 0.21$. A comparison with previous ARPES measurements[14] indicates that this signature is related to a Lifshitz transition, due to the disappearance of the inner hole FS at the **Γ** point. This change occurs at the same concentration at which SC is suppressed. Therefore, our findings seem to be in agreement with the proposal by Liu *et al.* that a necessary condition for SC might be a nonreconstructed central hole pocket, rather than a perfect nesting between the central and the corner pockets.[34] In order to draw a similar conclusion for the K-doped system, further investigations of its electronic structure are necessary; accordingly, ARPES measurements on our single crystals are already in progress.

ACKNOWLEDGMENT

This work was supported by the DFG through SPP 1458.

*jmaiwal@gwdg.de

[1]M. Norman, Science **332**, 196 (2011).
[2]N. Mathur, F. Grosche, S. Julian, I. Walker, D. Freye, R. Haselwimmer, and G. Lonzarich, Nature **394**, 39 (1998).
[3]H. S. Jeevan, Z. Hossain, D. Kasinathan, H. Rosner, C. Geibel, and P. Gegenwart, Phys. Rev. B **78**, 92406 (2008).
[4]T. Terashima, M. Tomita, M. Kimata, H. Satsukawa, A. Harada, K. Hazama, S. Shinya, Uji, H. Suzuki, T. Matsumoto, and K. Murata, J. Phys. Soc. Jpn. **78**, 083701 (2009).
[5]N. Kurita, M. Kimata, K. Kodama, A. Harada, M. Tomita, H. Suzuki, T. Matsumoto, K. Murata, S. Uji, and T. Terashima, *J. Phys. Conf. Ser.* **273**, 012098 (2011).
[6]Y. Qi, Z. Gao, L. Wang, D. Wang, X. Zhang, and Y. Ma, New J. Phys. **10**, 123003 (2008).
[7]Z. Ren, Q. Tao, S. Jiang, C. Feng, C. Wang, J. Dai, G. Cao, and Z. Xu, Phys. Rev. Lett. **102**, 137002 (2009).
[8]H. S. Jeevan, Z. Hossain, D. Kasinathan, H. Rosner, C. Geibel, and P. Gegenwart, Phys. Rev. B **78**, 052502 (2008).
[9]J. Herrero-Martín, V. Scagnoli, C. Mazzoli, Y. Su, R. Mittal, Y. Xiao, T. Brueckel, N. Kumar, S. K. Dhar, A. Thamizhavel, and L. Paolasini, Phys. Rev. B **80**, 134411 (2009).
[10]H.-H. Wen and S. Li, Annu. Rev. Condens. Matter Phys. **2**, 121 (2011).
[11]D. Johnston, Adv. Phys. **59**, 803 (2010).
[12]J. Paglione and R. Greene, Nature Phys. **6**, 645 (2010).
[13]H. S. Jeevan, D. Kasinathan, H. Rosner, and P. Gegenwart, Phys. Rev. B **83**, 054511 (2011).
[14]S. Thirupathaiah, E. D. L. Rienks, H. S. Jeevan, R. Ovsyannikov, E. Slooten, J. Kaas, E. van Heumen, S. de Jong, H. A. Dürr, K. Siemensmeyer, R. Follath, P. Gegenwart, M. S. Golden, and J. Fink, Phys. Rev. B **84**, 014531 (2011).
[15]D. Wu, G. Chanda, H. S. Jeevan, P. Gegenwart, and M. Dressel, Phys. Rev. B **83**, 100503 (2011).
[16]I. Paul and G. Kotliar, Phys. Rev. B **64**, 184414 (2001).
[17]H. Kondo, J. Phys. Soc. Jpn. **71**, 3011 (2002), and references therein.
[18]S. Zapf, D. Wu, L. Bogani, H. S. Jeevan, P. Gegenwart, and M. Dressel, Phys. Rev. B **84**, 140503 (2011).
[19]Quantum Design, *Physical Property Measurement System: Thermal Transport Option Users Manual*, 3rd ed. (Quantum Design, San Diego, CA, 2002).
[20]K. Kihou *et al.*, J. Phys. Soc. Jpn. **79**, 124713 (2010).
[21]M. Gooch, B. Lv, B. Lorenz, A. M. Guloy, and C. W. Chu, Phys. Rev. B **79**, 104504 (2009).
[22]F. J. Blatt, P. A. Schroeder, C. L. Foiles, and D. Greig, *Thermoelectric Power of Metals* (Plenum Press, New York, 1976).
[23]R. D. Barnard, *Thermoelectricity in Metals and Alloys* (Taylor & Francis, London, 1972).
[24]Z. Ren, Z. Zhu, S. Jiang, X. Xu, Q. Tao, C. Wang, C. Feng, G. Cao, and Z. Xu, Phys. Rev. B **78**, 052501 (2008).
[25]G. Wu, H. Chen, T. Wu, Y. Xie, Y. Yan, R. Liu, X. Wang, J. Ying, and X. Chen, J. Phys. Condens. Matter **20**, 422201 (2008).
[26]P. C. Canfield and S. L. Bud'ko, Annu. Rev. Condens. Mat. Phys. **1**, 27 (2010).
[27]L. Li *et al.*, New J. Phys. **11**, 025008 (2009).
[28]K. Sasmal, B. Lv, B. Lorenz, A. M. Guloy, F. Chen, Y.-Y. Xue, and C.-W. Chu, Phys. Rev. Lett. **101**, 107007 (2008).
[29]B. Lv, Ph.D. thesis, University of Houston, 2009.
[30]Q. Tao, Z. Zhu, X. Lin, G. Cao, Z. Xu, G. Chen, J. Luo, and N. Wang, J. Phys. Condens. Matter **22**, 072201 (2010).
[31]D. J. Singh, Phys. Rev. B **78**, 94511 (2008).
[32]B. Lv, M. Gooch, B. Lorenz, F. Chen, A. Guloy, and C. Chu, New J. Phys. **11**, 025013 (2009).
[33]H. Hodovanets, E. D. Mun, A. Thaler, S. L. Budko, and P. C. Canfield, Phys. Rev. B **83**, 094508 (2011).
[34]C. Liu, A. D. Palczewski, R. S. Dhaka, T. Kondo, R. M. Fernandes, E. D. Mun, H. Hodovanets, A. N. Thaler, J. Schmalian, S. L. Bud'ko, P. C. Canfield, and A. Kaminski, Phys. Rev. B **84**, 020509 (2011).